Extended Abstracts of the 2005 International Conference on Solid State Devices and Materials, Kobe, 2005, pp.58-59

C-1-5

Electrical Characteristics of Porous Zeolite Interlayer Dielectrics

Takenobu Yoshino[1], Guoqing Guan[2], Nobuhiro Hata[1], Nobutoshi Fujii[3] and Takamaro Kikkawa[1,4]

[1]MIRAI, Advanced Semiconductor Research Center (ASRC), National Institute of Advanced Industrial Science and Technology (AIST), and [2]ASRC, AIST, Tsukuba, 305-8569, Japan.
[3]MIRAI, Association of Super-Advanced Electronics Technology (ASET), Tsukuba, 305-8569, Japan
[4]Research Center for Nanodevices and Systems (RCNS), Hiroshima University, Higashi-Hiroshima, 739-8527, Japan.

1 Introduction

Recently, all-silica zeolite films have been paid much attention as an advanced low-dielectric-constant (low-*k*) interlayer dielectrics with a lower *k* value and higher mechanical strength. Zeolite-based low-*k* film is clearly distinguished from conventional silica low-*k* films with amorphous network, *i.e.*, the skeletal structure of the zeolite-based film consists of locally ordered crystalline silica [1–3]. In zeolite low-*k* films, the research had been mainly subjected to the mechanical strength and lower *k* value, while electrical properties were hardly studied because samples were prepared without purification of reagents. In this paper, we synthesized ultra-pure zeolite using pre-purified reagents and studied the leakage current mechanism of porous zeolite films.

2 Experimental

MEL-type zeolite as shown in Fig. 1 was prepared by hydrothermal synthesis of TBAOH (tetra-butyl ammonium hydroxide), TEOS (tetraethyl orthosilicate) and EtOH (ethyl alcohol) mixture at 100°C. TBAOH was pre-purified using ion-exchange resin, and TEOS and EtOH in semiconductor grades were used. The radiofrequency inductively coupled plasma (ICP) mass analysis supported that the suspension contained metal elements less than 10 ppb. After butanol and surfactant as a pore-generator were added to the suspension, zeolite film was formed by spin coating on Si wafers followed by calcination at 400°C.

For electrical measurements, a metal-insulator-semiconductor (MIS) capacitor was fabricated by evaporating metal electrodes with circular-hole mask. Current density J as a function of applied electric field E (J-E relation) were measured at various temperatures. To avoid moisture adsorption and oxidation of Al electrodes, the measurements were performed under dry nitrogen atmosphere.

3 Results and Discussion

Figure 2(a) shows Fourier transform infrared spectrum (FT-IR) for the fabricated zeolite film. A small peak was found at around 550 cm^{-1}, which was the evidence of the asymmetric stretching mode in five-membered ring blocks in MEL-type zeolite crystal [4,5]. The other two peaks at 800 and 400 cm^{-1} are characteristic vibration mode of Si-O-Si bonds [5]. Pore size distribution analyzed from small x-ray scattering spectrum is shown in Fig. 2(b), from which the mesopore size induced by the surfactant was estimated to be around 1.9 nm.

The value of the dielectric constant k of fabricated zeolite film was 2.1 after drying at 300°C in nitrogen atmosphere. The k value was decreased down to 1.8 after a sililation treated with TMCTS (1, 3, 5, 7-tetramethyl-cyclotetrasiloxane) [6, 7]. The mechanical strength was also improved by the TMCTS treatment from 2.5 GPa to 5.1 GPa. The leakage current with a TMCTS treated sample also decreased to as low as 5×10^{-12} A/cm^2 at 1 MV/cm as shown in Fig. 3.

The J-E relation measured at elevated temperatures for zeolite are plotted in Fig. 4. Current density J increased by 2–3 orders of magnitude from 100°C to 300°C. For zeolite samples measured at elevated temperatures, TMCTS treatment was not performed. Therefore the measurements were carried out above 100°C to avoid moisture adsorption.

To understand a conduction mechanism for porous zeolite film, $\ln J$ is plotted as a function of $E^{1/2}$ as shown in Fig. 5. Above 0.5–1 MV/cm, $\ln J$ is proportional to $E^{1/2}$. When we assume Schottky emission (SE) model, current density J_S is expressed as

$$J_S = A^* T^2 \exp\left(\beta_S \sqrt{E} - q\phi_S\right)/k_B T, \tag{1}$$

where A^* is the Richardson constant, q is the electric charge, k_B is the Boltzman constant, and $\beta_S = q\sqrt{q/4\pi\varepsilon}$, $\varepsilon = k\varepsilon_0$ is dielectric constant of low-k film [8]. From the slope in Fig. 5 above 1 MV/cm, the value of β_S in the unit of 10^{-23} J/(cm/V)$^{1/2}$ was estimated to be about 4. By using $k = 2.1$ for present zeolite sample, theoretical value of $\beta_{S,\mathrm{calc}}$ also becomes 4, while β for Pool-Frenkel (PF) model expressed as $\beta_{PF,\mathrm{calc}} = q\sqrt{q/\pi\varepsilon}$ is calculated as 8. Therefore, the conduction for zeolite follows SE model rather than PF model. The Schottky barrier height ϕ_S of the zeolite was estimated to be about 1 eV from the slope of J/T^2 versus T^{-1} as shown in Fig. 6.

Similar measurements were also carried out for amorphous-network porous silica with non-periodic pores (disordered pore structure film). Figure 7 shows J-E curves of the disordered film. The value of β is also 4 above 3 MV/cm and 200°C, indicating the disordered film is controlled also by SE type conduction above 3 MV/cm and 200°C. The barrier height was estimated to be 1 eV from the linear region in Fig. 9 above 200°C.

As described above, SE type conduction with $\phi_S \sim 1$ eV was found for both zeolite and disordered films. This means the conduction mechanism at higher fields is equivalent for zeolite and disordered films, although breakdown field for zeolite film is approximately 2/3 of that for disordered film. In other words, SE governs the conduction for both zeolite and disordered films under higher electric field near breakdown at high temperature. J-E curves for the disordered film measured below 200°C were essentially unchanged. Furthermore, field dependences of the disordered film was also weak below 2 MV/cm. In these fields and temperatures regions, the conduction was not attributed to SE model as well as PF model. In the case of present zeolite films, J exhibited relatively strong temperature and field dependences even at low temperatures and low fields. Namely, field-assisted current leakage was remarkable in zeolite film, indicating relatively shallow trapping levels existed in the zeolite bandgap. By taking into account of weak peak intensity at 550 cm^{-1} in FT-IR spectrum shown in Fig. 2(a), local defects in the crystalline network of zeolite may affect on the temperature dependent current leakage. Further optimization of sample preparation process for well-ordered framework is needed.

4 Summary

MEL-type zeolite films were successfully synthesized from purified precursor solutions, and the uniform low-k film was formed on Si wafers. The leakage current of zeolite films measured at room temperature was as low as 5×10^{-12} A/cm^2 at 1 MV/cm. Temperature dependences of J-E relation suggested that the conduction mechanism of the zeolite film at elevated temperatures were well explained by SE model above 1 MV/cm with a barrier height of approximately 1 eV. This value was comparable with disordered porous silica film, indicating the conduction mechanism near the breakdown field was equivalent for pure-silica zeolite and disordered porous silica.

Zeolite is also a promising candidate for advanced low-k materials, while its performance under elevated temperatures should be improved by decreasing of local defects in the crystalline network of zeolite.

Acknowledgments

This work was supported by NEDO. JST was acknowledged for Cooperative System for Supporting Priority Research.

References

[1] Z. Wang, H. Wang, A. Mitra, L. Huang, and Y. Yan: Adv. Mater. **13** (2001) 746.

[2] S. Li, Z. LKi, and Y. Yan: Adv. Mater. **15** (2003) 1528.

[3] O. Larlusa, S. Mintovab, V. Valtcheva, B. Jeanc, T. H. Metzgerc, and T. Beinb: Appl. Surf. Sci. **226** (2004) 155.

[4] J. Dong, J. Zou, and Y. Long: Microporous and Mesoporous Materials **57** (2003) 9.

[5] G. Coudurier, C. Naccache and J.C. Vedrine: J. Chem. Soc., Chem. Commun. (1982) 1413.

[6] Y. Oku et al., *2003 IEEE Inter. Elec. Dev. Meet., Tech. Digest*, (IEEE, Washington D. C., 2003) p. 139.

[7] K. Kohmura, S. Oike, M. Murakami, H. Tanaka, S. Takada, Y. Seino, and T. Kikkawa: Mat. Res. Soc. Symp. Proc. **812** (2004) F6.2.1.

[8] S. M. Sze, *Physics of Semiconductor Devices* 2nd ed., (Wiley, New York, 1981).

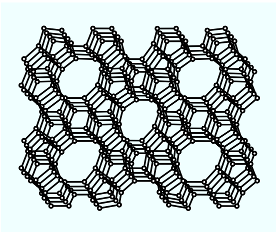

Fig. 1 MEL type zeolite structure view from <100> direction.

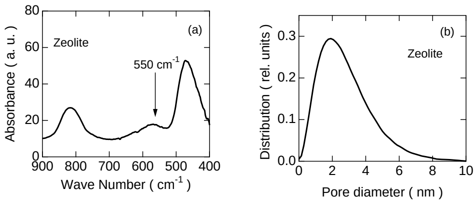

Fig. 2 Fourier transform infrared spectrum (a) and pore size distribution determined by small angle x-ray scattering (b) for the zeolite film.

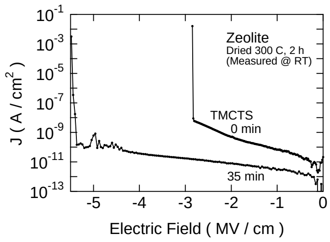

Fig. 3 J-E relation for zeolite films with and without TMCTS treatment.

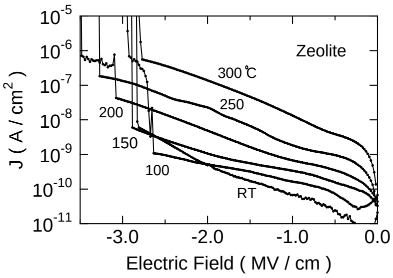

Fig. 4 J-E relation of zeolite low-k films at elevated temperatures.

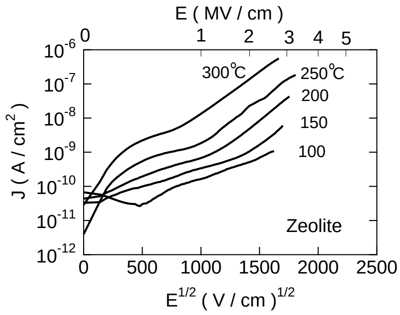

Fig. 5 $\ln J$ versus $\sqrt{E}$ according to eq. 1

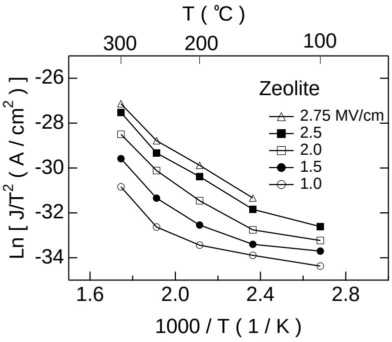

Fig. 6 Plot of $\ln J$ as a function of inverse temperature.

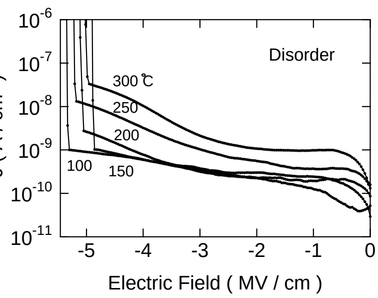

Fig. 7 J-E relations of disordered porous silica films measured at different temperatures.

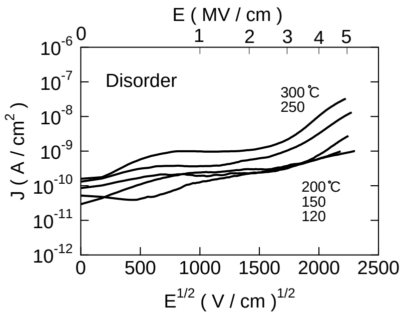

Fig. 8 $\ln J$ versus $\sqrt{E}$ for disordered porous silica.

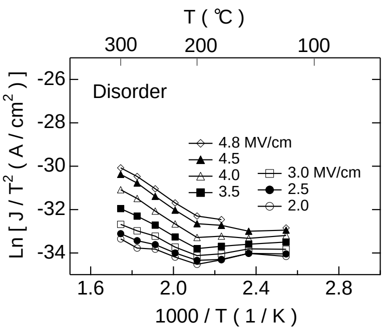

Fig. 9 $\ln J$ versus T^{-1} for disordered porous silica.